Supporting Information

Oligomer-Engineered Active Layer Enables High-Performance Semi-Transparent Organic Photovoltaics

Xinyuan Ren[a#], Yunhui Xie[a#], Xuexiang Huang[b*], Feiyan Wu[a], Jiabin Liu[a], Hyeong Hui Kim[c], Han Young Woo[c*], Junying Xu[a*], Bin Huang[d], and Lie Chen[a]

a. College of Chemistry and Chemical Engineering/Film Energy Chemistry for Jiangxi Provincial Key Laboratory (FEC), Nanchang University, Nanchang 330031, Jiangxi, China.

b. College of Intelligent Manufacturing and Materials Engineering, Gannan University of Science and Technology, 156 Kejia Avenue, Ganzhou, Jiangxi 341000, China.

c. Department of ChemistryCollege of ScienceKorea University145 Anam-ro, Seongbuk-gu, Seoul 02841, Republic of Korea.

d. School of Chemistry and Chemical Engineering Jiangxi University of Science and Technology, 156 Ke Jia Avenue, Ganzhou, 34100, P. R. China.

Corresponding author: Dr. Xuexiang Huang, Dr. Junying Xu, and *Prof*. Dr. Han Young Woo.

Email: 649498323@qq.com (X. Huang), hywoo@korea.ac.kr (H. Woo), and xujunying@ncu.edu.cn (J. Xu).

[#]*These authors contributed equally to this work.*

Materials and synthesis

PTB7-Th-2F were synthesized in our previous work, Y6, BDT and F-TT were purchased from Derthon Optoelectronic Materials Science Technology Co LTD (Shenzhen, China). The synthetic processes of oligomer small molecules XY-1 was provided in **Figure S1**. The synthesis of XY-1 is as follows:

(1) BDT (184.48mg, 0.3mmol), THF(4.0ml) in nitrogen atmosphere in a 50 ml double-necked flask with condenser. Mix the mixture for 0.5h at -73℃.

(2) Add drop by drop the n-BuLi (0.14ml, 0.36mmol) into the above reactions， continue the reaction for 30 min at -73℃.

(3) After the reaction, it was activated in air for 2 hours, then put it into the low-temperature reaction tank again, and after a few minutes, 0.3ml of trimethyltin chloride was added and reacted at -73 ℃ for 2h. After that, water was added for separation, and the target product was obtained by rotary steaming.

(4) The above product is sucked into a 50ml double-necked glass reaction flask with a rubber head dropper, F-TT (141.67mg, 0.3mmol) and $Pd(PPH_3)_4$ (27.73mg, 0.0024mmol) are added to the reaction flask, toluene is added to dissolve it in nitrogen conditions and reacted at 110 ℃ for 4~5h, it is quenched with water, and then separated for liquid treatment. After rotary steaming, the silica gel column was wet loaded and the column was processed to obtain the final product-XY-1.

Measurements

Optical characterizations. UV-vis absorption spectra were recorded on an Agilent series UV-Vis-NIR spectrophotometer. All film samples were spin-cast on quartz slice substrates. The photoluminescence spectra (PL) were measured by photoluminescence spectroscopy (Hitachi F-7000).

Electrochemical characterizations. Cyclic voltammetry (CV) was performed by a Zahner IM6e electrochemical workstation, using Ag/AgCl as the reference electrode, a Pt plate as the counter electrode, and a glassy carbon as the working electrode. Polymers were drop-cast onto the electrode from chloroform solutions to form thin films. 0.1 mol L-1 tetrabutylammonium hexafluorophosphate in anhydrous acetonitrile was used as

the supporting electrolyte. The scan rate was 0.05 V s^{-1}. The E_{HOMO} and E_{LUMO} are calculated as referring to the eqs (1) and (2).

$$E_{HOMO}=-(Eox+4.4)\ eV\ (1),$$

$$E_{LUMO}=-(Ered+4.4)\ eV\ (2).$$

Surface energy characterization. The water contact angle images of neat films were recorded by using a KRÜSS DSA 100 instrument under atmospheric condition.

DSC measurements. DSC was measured by TA DSC Q2000 differential scanning calorimeter, with the samples being heated to 300 °C and then cooled to 40 °C at a heating/cooling rate of 10 °C/min.

AFM characterizations. The specimen for AFM measurements was prepared using the same procedures for fabricating devices but without PDINO/Ag on top of the active layer.

Device Fabrication and Characterizations.

(1) Opaque device fabrication

The device is fabricated with ITO/ PEDOT: PSS/active layer/PDINN/Ag tradition structure. The ITO coated glass substrates were cleaned by ultrasound for 15 minutes in sequence in water/detergent, water, acetone and isopropanol, and then treated in ultraviolet ozone for 1400 seconds. The PEDOT: PSS solution was spin-coated on top of the cleaned ITO-coated glass substrate and the PEDOT: PSS film thickness was approximately 25 nm. After annealing at 150 °C for 20 min, then the substrates were transferred into a glove box. For the solar cells based on a BC operating condition, PTB7-Th-2F: Y6 :XY-1(1:2:0%，1%，2%，5% and 10%，w/w/w) mixture was dissolved in chloroform (CF) with a donor concentration of 5.33 mg/ml, and 1,8-diiodooctane (DIO) and CN was added (volume ratio 0.25% and 0.25%, respectively). The solution is stirred at 40℃ for 10 hours and then spin-coated on the surface of PEDOT:PSS layer in a glove box in nitrogen-based atmosphere (3000r 40s). After annealing at 100 °C for 10 min. The PDINN was dissolved in methanol at 1 mg mL^{-1} and spin-coated on active layer at 3000 rpm for 30s. Finally, 90-nanometer thick Ag

layers were deposited on the active layer under high vacuum of ~3×10^{-4}Pa. The overlapping area of cathode and anode was 4 square millimeters. *J-V* curves of devices based on PTB7-Th-2F: Y6: different ratios of XY-1 were measured under the standard AM 1.5G spectrum of 100 MW cm^{-2}.

(2) Semitransparent device fabrication

The device is fabricated with ITO/PEDOT: PSS/active layer/PDINN/Ag tradition structure. The ITO coated glass substrates were cleaned by ultrasound for 15 minutes in sequence in water/detergent, water, acetone and isopropanol, and then treated in ultraviolet ozone for 1400 seconds. The PEDOT: PSS solution was spin-coated on top of the cleaned ITO-coated glass substrate and the PEDOT: PSS film thickness was approximately 25 nm. After annealing at 150 °C for 20 min, then the substrates were transferred into a glove box. PTB7-Th-2F: Y6 :XY-1(1:2:0%，1%，2%，5% and 10%，w/w/w) mixture was dissolved in chloroform (CF) with a donor concentration of 5.33 mg/ml, and 1,8-diiodooctane (DIO) and CN was added (volume ratio 0.25% and 0.25%, respectively). The solution is stirred at 40℃ for 10 hours and then spin-coated on the surface of PEDOT:PSS layer in a glove box in nitrogen-based atmosphere (3000r, 40s). Finally, 15nm thickness Ag and layers were deposited on the active layer under high vacuum of ~3x10^{-4}Pa. Then, MoO_3 (35 nm) were evaporated onto the surface of Ag. The overlapping area of cathode and anode was 4 square millimeters. *J-V* curves of ST-OSC devices were measured under the standard AM 1.5G spectrum of 100 MW cm^{-2}.

Photon balance in ST-OSC. Apparently, photon balance (at every wavelength) must be considered in reporting the performance of ST-OSC. The sum of absorption (A), transmission (T) and reflection (R) of the device should be equal to 1 at every wavelength. Owing to difficulties in measuring A directly, the minimum absorption can be estimated from the EQE. Thus, the sum of EQE, T, and R should be less than unity at every wavelength.

$$E(\lambda) + T(\lambda) + R(\lambda) \leq 1 \qquad E(\lambda) + A(\lambda) + R(\lambda) \leq 1 \qquad \text{(Eq. S1)}$$

AVT test. Firstly, we tested the power conversion efficiency (PCE) of the prepared semi-transparent devices and selected the device with the best PCE under each

condition for immediate transmittance testing. After completing the tests, we recorded the transmittance values corresponding to the wavelength range from 390nm to 740nm in a table. The final average visible transmittance (AVT) value was then calculated through weighted averaging.

Electron and Hole mobility measurements. Hole and electron mobilities were measured using the space charge limited current (SCLC) method, with hole-only device ITO/poly(3,4-ethylenedioxythiophene): poly(styrenesulfonate) (PEDOT: PSS)/ active layer /MoO_3/Ag for hole mobility measurement and the electron-only devices used a diode configuration of ITO/ZnO/activel ayer/PDINO/Al by taking current-voltage curve in the range of -5~5 V. The SCLC mobilities were calculated by MOTT-Gurney equation, which is described by: $J = 9\varepsilon_0\varepsilon_r u V^2 / 8L^3$, where J is the current density, L is the film thickness of active layer, ε_0 is the permittivity of free space (8.85×10^{-12} F m^{-1}), ε_r is the relative dielectric constant of the transport medium, u is the hole or electron mobility, V is the internal voltage in the device and $V = V_{appl}-V_r-V_{bi}$, where V_{appl} is the applied voltage to the device, V_r is the voltage drop due to contact resistance and series resistance across the electrodes, and V_{bi} is the built-in voltage due to the relative work function difference of the two electrodes.

Detailed V_{loss} measurements. Highly Sensitive EQE was measured by using an integrated system (PECT-600, Enlitech), where the photocurrent was amplified and modulated by a lock-in instrument. The-FTPS-spectra-were-calibrated by a germanium detector. Electroluminescence (EL) quantum efficiency (EQE_{EL}) measurements were performed by applying external voltage/current sources through the-devices (REPS, Enlitech). EQE_{EL} measurements were carried out from 0 to 3 V. Details of optical E_{gap} determination. The EQE is interpreted as a superposition of distribution of step functions with a step at E_{gap} having a certain probability distribution. This probability distribution can be obtained from the derivative dEQE/dE. The part where the probability is greater than half of the maximum is integrated to get an average bandgap.

GIWAXS measurements. The GIWAXS measurement was carried out at the PLS-II 6A U-SAXS beamline of the Pohang Accelerator Laboratory in Korea. The X-rays coming from the in-vacuum undulator (IVU) were monochromate (wavelength l =

1.10994 Å) using a double crystal monochromator and focused both horizontally and vertically (450 (H) x 60 (V) um2 in FWHM @ the sample position) using K-B type mirrors. The grazing incidence wide-angle X-ray scattering (GIWAXS) sample stage was equipped with a 7-axis motorized stage for the fine alignment of the sample, and the incidence angles of the X-ray beam were set to be 0.11°-0.13° for the neat and blend films. The GIWAXS patterns were recorded with a 2D CCD detector (Rayonix SX165) and an X-ray irradiation time within 100 s, depending on the saturation level of the detector. Diffraction angles were calibrated using a sucrose standard (monoclinic, P21, a=10.8631Å, b =8.7044 Å, c=7.7624 Å, and b=102.938 Å) and the sample-to-detector distance was ~231 mm.

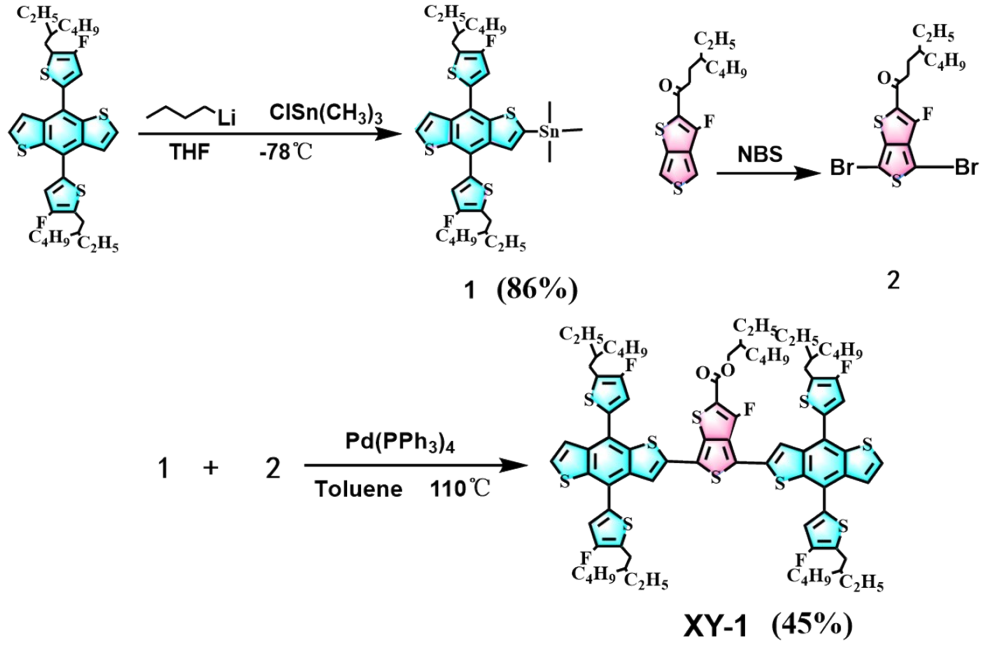

Fig. S1 The detailed synthesis process of XY-1.

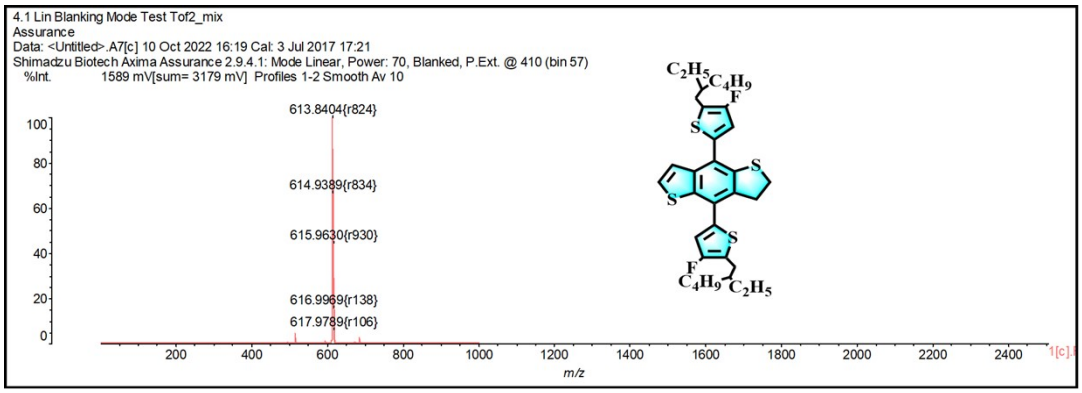

Fig. S2 The BDT unit removes the MS of one hydrogen atom.

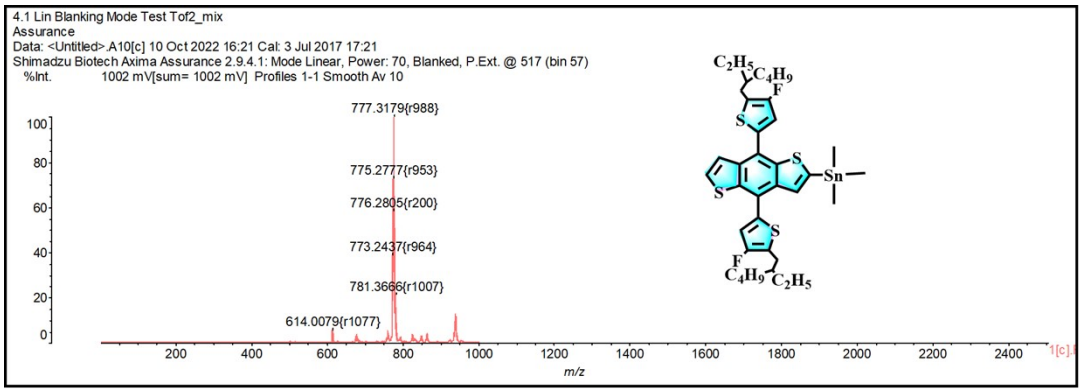

Fig. S3 MS of Product 1.

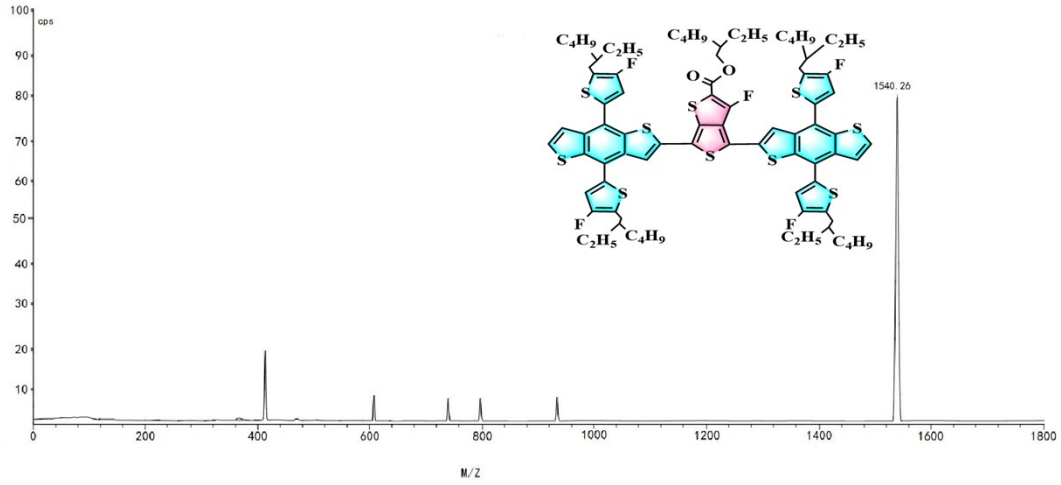

Fig. S4 MS of XY-1.

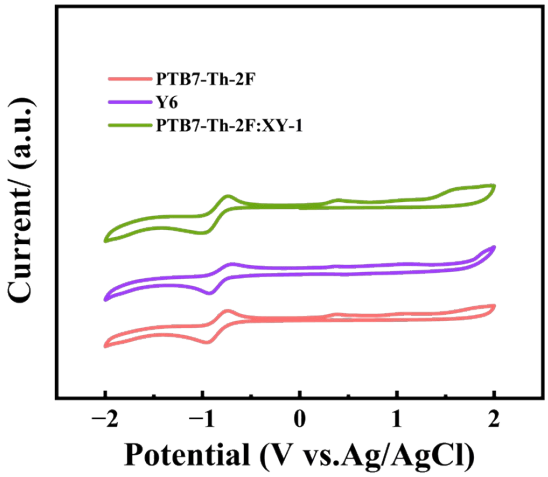

Fig. S5 The cyclic voltammetry measurements of PTB7-Th-2F, Y6, XY-1 and PTB7-Th-2F: 5%XY-1.

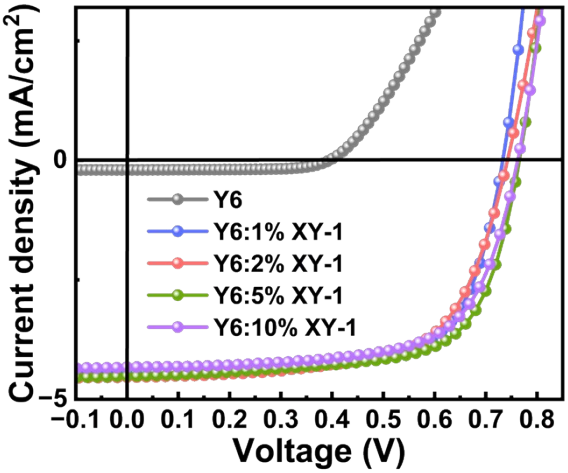

Fig. S6 *J*−*V* curves of oligomer: Y6-based devices.

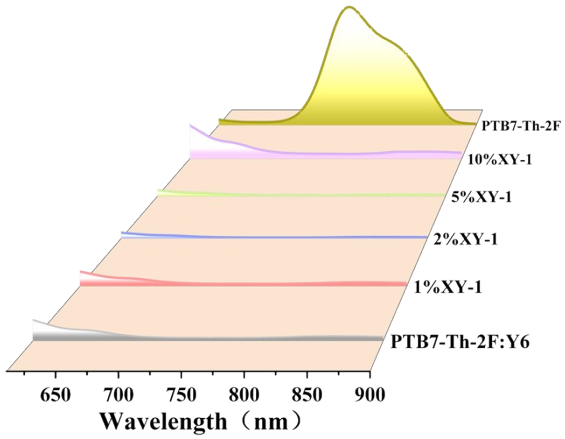

Fig. S7 Photoluminescence (PL) spectra of the neat film of PTB7-Th-2F and the five blend films of PTB7-Th-2F:Y6, PTB7-Th-2F:Y6(1% XY-1), PTB7-Th-2F:Y6(2% XY-1), PTB7-Th-2F:Y6(5% XY-1) and PTB7-Th-2F:Y6(10% XY-1).

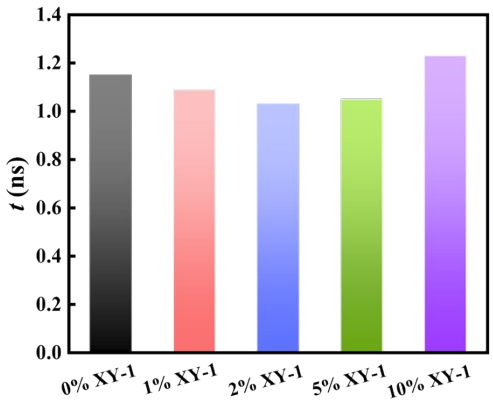

Fig. S8 The hole transfer rates of films are determined by time-resolved PL decay spectra.

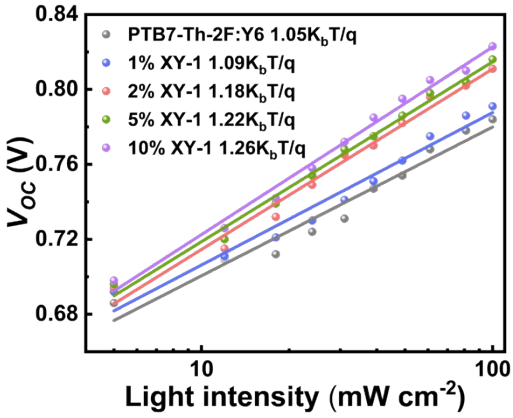

Fig. S9 Light intensity dependence of V_{OC}.

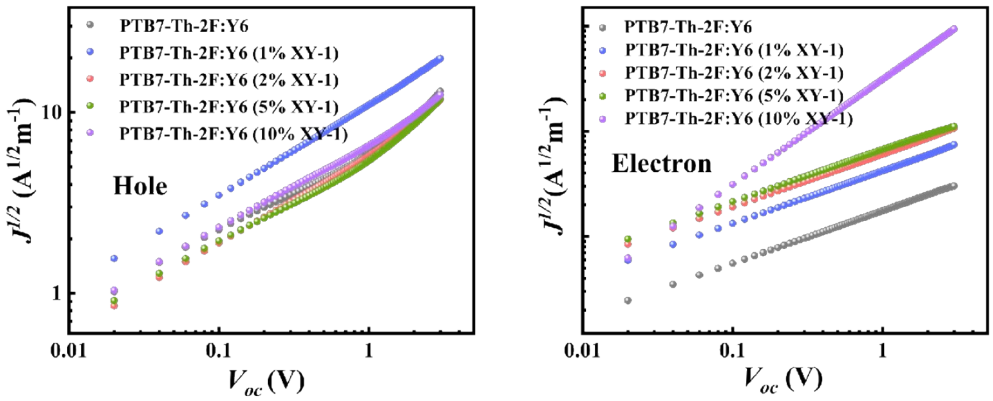

Fig. S10 Hole and Electron mobility of optimized devices measured by SCLC**.**

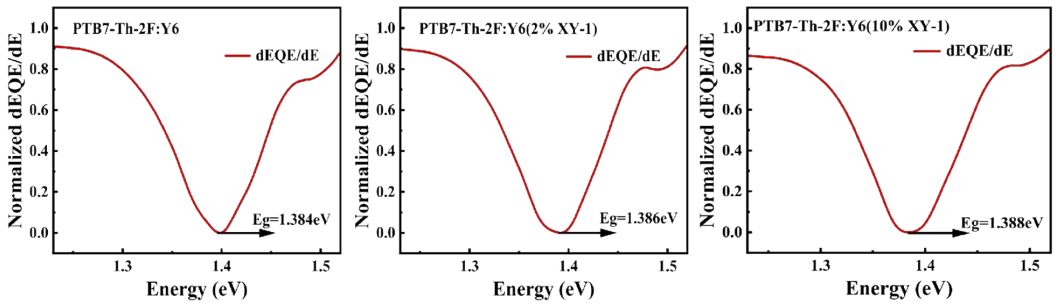

Fig. S11 The EQE spectrum (dEQE/dE) of optimized devices of PTB7-Th-2F:Y6, PTB7-Th-2F:Y6(2% XY-1) and PTB7-Th-2F:Y6(10% XY-1).

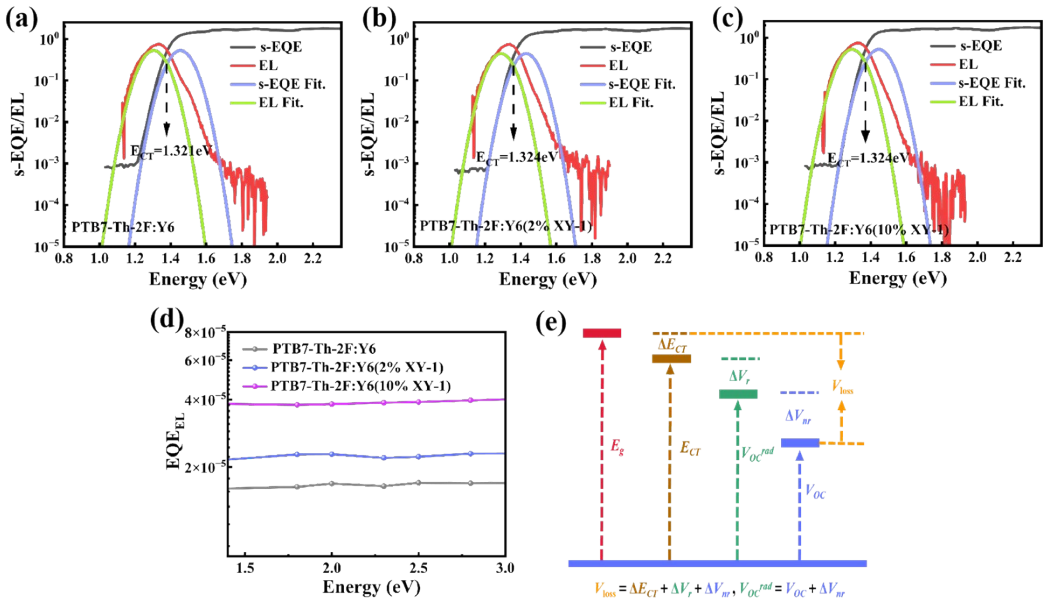

Fig. S12 (a-c) Reduced sEQE, EL spectra and (d) EQE_{EL} of PTB7-Th-2F:Y6, PTB7-Th-2F:2%XY-1: Y6 and PTB7-Th-2F:10%XY-1: Y6 based devices. (e) Voltage loss related parameters diagram.

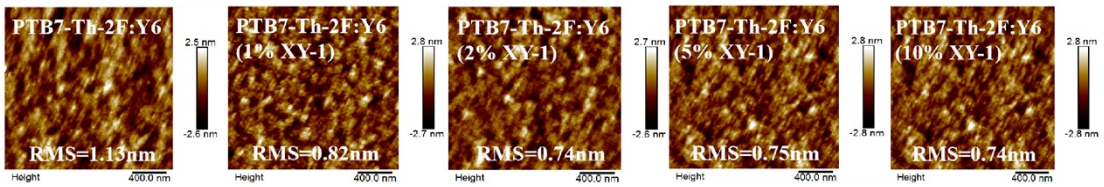

Fig. S13 AFM height images of the related blend films.

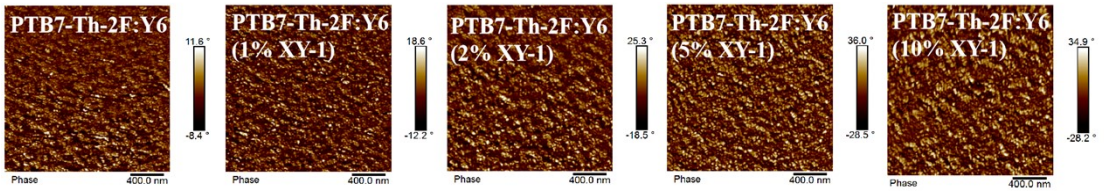

Fig. S14 AFM phase images of the related blend.

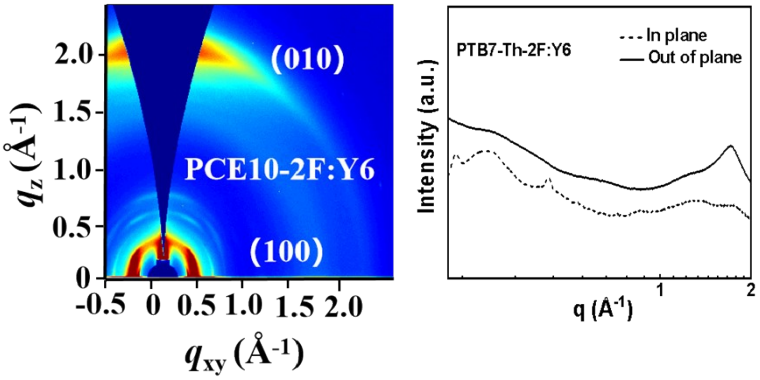

Fig. S15 2D and 1D GIWAXS patterns of PTB7-Th-2F:Y6.

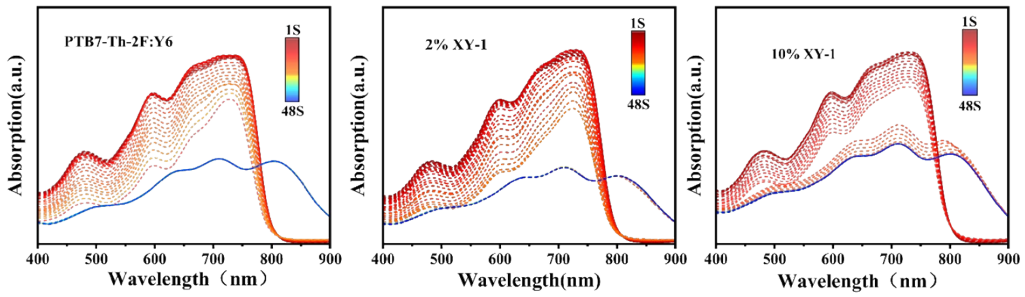

Fig. S16. The original in-situ UV-Vis absorption curves of blend films with different ratios of PTB7-Th-2F: Y6: XY-1.

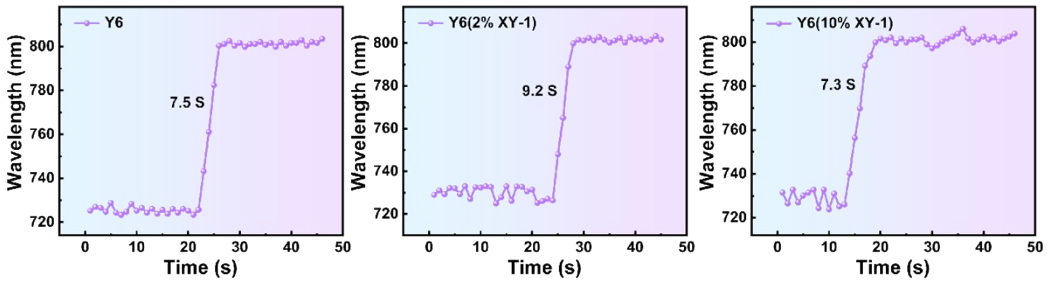

Fig. S17 Time evolution of acceptor peak positions of blend films.

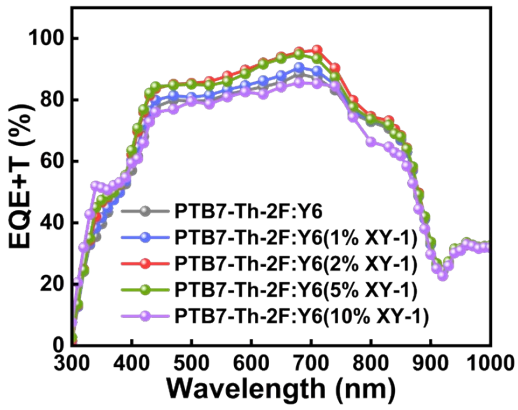

Fig. S18 EQE+T versus wavelength of blend films with different ratios of PTB7-Th-2F: Y6: XY-1.

Table S1. PCE of opaque and semi-transparent OSCs reported in literatures with all-narrow band gap BHJ systems.

Devices	Opaque OSCs		Semi-transparent OSCs		Reference
	PCE (%)	V_{OC} (V)	PCE (%)	LUE (%)	
PTB7-Th-2F: Y6: XY-1	14.49	0.811	12.00	5.01	This work
PTB7-Th:H3	12.30	0.720	8.38	4.06	[1]
PCE10-BDT2F-0.8: Y6	13.80	0.753	10.85	4.46	[2]
PTB7-Th: ATT-9	11.37	0.674	7.34	3.73	[3]
PTB7-Th：IEICO-4F	11.60	0.690	8.10	1.87	[4]
PTB7-Th: ATT-9	13.35	0.663	9.37	3.33	[5]
PTB7-Th: BZO-4Cl	14.12	0.706	9.33	4.02	[6]
PTB7-Th: A078	13.40	0.760	11.60	2.90	[7]
PTB7-Th: $PC_{71}BM$	10.00	0.791	6.91	1.87	[8]
PTB7-Th:BT-CIC	11.60	0.710	7.20	3.20	[9]
PCE10-2Cl: IT-4F	10.72	0.822	9.00	2.72	[10]
PTB7-Th: IEICO-4Cl	10.30	0.727	7.47	2.38	[11]

Devices	Opaque OSCs		Semi-transparent OSCs		Reference
	PCE (%)	V_{OC} (V)	PCE (%)	LUE (%)	
PTB7-Th: IEICS-4F	10.30	0.750	7.50	2.63	[12]
PTB7-Th:CO,8DFIC: IEICO-4F	11.94	0.714	8.23	1.71	[13]
PTB7-Th: BDTThIT-4F: IEICO-4F	12.03	0.737	9.40	2.31	[14]
PTB7-Th: FNIC2	13.00	0.741	9.51	1.94	[15]
PTB7-Th: FOIC	12.00	0.743	10.30	3.86	[16]
PCE-10: BT-CIC: TT-FIC	11.70	0.690	8.20	3.67	[17]
PCE10: ICBA: Y8	12.86	0.742	10.46	2.78	[18]
PTB7-Th: ACS8	13.20	0.751	9.40	4.06	[19]
PTB7-Th:PC71BM: FOIC	12.32	0.753	9.67	4.87	[20]
PTB7-Th: J71: IHIC	10.35	0.780	8.93	2.31	[21]

Table S2. Information from the top surface measured by water contact angle.

Materials	Contact（Water）	Surface energy （mN/m）	Blend film	γ D-A (mN m^{-1})
PTB7-Th-2F	106.18	19.32	PTB7-Th-2F:Y6	0.42
Y6	96.06	25.46	Y6: XY-1	0.31
XY-1	104.79	20.15	PTB7-Th-2F: XY-1	0.0087

Table S3. Photovoltaic parameters of XY-1: Y6-based OSCs under AM 1.5G 100 mW cm-2 illumination.

Active Layer	V_{OC} (V)	J_{SC} (mA cm-2)	*FF* (%)	PCE (%)
Y6	0.394	0.202	26.39	0.020
Y6:1%XY-1	0.732	4.448	29.95	0.973
Y6:2% XY-1	0.741	4.536	32.68	1.095
Y6:5% XY-1	0.764	4.518	31.23	1.075
Y6:10% XY-1	0.773	4.327	27.99	0.932

Table S4. The parameters of exciton dissociation efficiency and charge collection efficiency. And hole and electron mobilities of PTB7-Th-2F: XY-1: Y6 (D/A from 1:0:2 to 1:10%:2).

Devices	Oligomer	μ_h (cm^2 V^{-1} s^{-1})	μ_e (cm^2 V^{-1} s^{-1})	μ_h/μ_e
PTB7-Th-2F: Y6: XY-1	0	8.59×10^{-4}	6.32×10^{-4}	1.36
	1%XY-1	8.67×10^{-4}	6.72×10^{-4}	1.29
	2%XY-1	9.03×10^{-4}	8.52×10^{-4}	1.06
	5%XY-1	8.84×10^{-4}	7.43×10^{-4}	1.19
	10%XY-1	8.31×10^{-4}	5.69×10^{-4}	1.46

Table S5. Detailed energy loss of opaque devices based on PTB7-Th-2F:Y6, PTB7-Th-2F:Y6:2%XY-1, and PTB7-Th-2F:Y6:10%XY-1.

active layer	E_g (eV)	E_{CT} (eV)	ΔE_{CT} (eV)	EQE_{EL}	V_{OC}^{rad} (V)	ΔV_{nr} (eV)	ΔV_r (eV)	V_{loss} (V)
PTB7-Th-2F:Y6	1.384	1.321	0.063	1.584×10^{-5}	1.072	0.286	0.249	0.598
PTB7-Th-2F:Y6 (2% XY-1)	1.386	1.324	0.062	2.076×10^{-5}	1.090	0.279	0.234	0.575
PTB7-Th-2F:Y6 (10% XY-1)	1.388	1.324	0.061	3.852×10^{-5}	1.086	0.263	0.238	0.562

Table S6. The location of (010) and (100) peaks, *d*-spacing, FWHM and CCL of the blend films.

Devices	Out-of-Plane				In-Plane			
	π-π stacking cell axis (010)				Unit cell long axis (100)			
	Q ($Å^{-1}$)	d-spacing (Å)	FWHM ($Å^{-1}$)	Coherence length(Å)	q($Å^{-1}$)	d-spacing (Å)	FWHM ($Å^{-1}$)	Coherence length(Å)
PTB7-Th-2F:Y6	1.709	3.675	0.359	17.493	0.213	29.484	0.104	60.385
PTB7-Th-2F: Y6 (1% XY-1)	1.711	3.670	0.341	18.416	0.251	25.020	0.101	62.187
PTB7-Th-2F: Y6 (2% XY-1)	1.732	3.626	0.290	21.655	0.213	29.484	0.082	76.585
PTB7-Th-2F: Y6 (5% XY-1)	1.724	3.643	0.333	18.884	0.264	23.788	0.091	69.010
PTB7-Th-2F: Y6 (10% XY-1)	1.707	3.680	0.408	15.392	0.262	23.969	0.104	60.385

Table S7. Detailed parameter on state-of-the-art ST-OSC devices without complex optical engineering reported in the literature

Reference	AVT (%)	PCE (%)	LUE (%)
[22]	28.85	11.74	3.39
[23]	33.8	8.1	2.74
[24]	20.98	12.58	2.64
[1]	50.09	8.38	4.06
	18.47	12.2	2.25
	27.9	8.22	2.29
[2]	41.08	10.85	4.46
[25]	40.4	10.1	4.00
[26]	25.9	13.15	3.41
[27]	37.31	11.71	4.37
[3]	50.8	7.34	3.73
[4]	23	8.1	1.84
[28]	30	11.3	3.39
[29]	30.52	11.68	3.56
[5]	35.5	9.37	3.33

Reference	AVT (%)	PCE (%)	LUE (%)
[30]	22.2	14.0	3.11
[31]	22.3	12.01	2.68
[6]	43.08	9.33	4.02
[32]	42.98	11.10	4.77
[33]	50.05	10.01	5.01
[34]	23.69	13.38	3.17
	36.57	12.25	4.48
[35]	45.61	11.18	5.10
	31.35	12.95	4.06
[36]	35.0	11.0	3.85
[37]	25.2	7.3	1.84
[19]	28.6	11.1	3.17
[38]	27.6	9.1	2.51
[39]	52	4.2	2.18
[21]	21.4	9.3	2.01
[40]	28.6	10.2	2.92
[41]	22.35	13.1	2.93
[42]	22.58	13.49	3.05

Reference	AVT (%)	PCE (%)	LUE (%)
[43]	21.4	13	2.78
[44]	26.56	10.46	2.78
[45]	20.2	13.02	2.63
[11]	33	8.25	2.72
[46]	43.3	5.9	2.55
[47]	21.6	14.0	3.02
This work	41.76	12.0	5.01

References

[1] Y. Li, C. He, L. Zuo, F. Zhao, L. Zhan, X. Li, R. Xia, H. L. Yip, C. Z. Li, X. Liu, H. Chen, *Adv. Energy Mater.* **2021**, 11, 2003408.

[2] X. Huang, L. Zhang, Y. Cheng, J. Oh, C. Li, B. Huang, L. Zhao, J. Deng, Y. Zhang, Z. Liu, F. Wu, X. Hu, C. Yang, L. Chen, Y. Chen, *Adv. Funct. Mater.* **2021**, 32, 2108634.

[3] S. Sun, W. Zha, C. Tian, Z. Wei, Q. Luo, C. Q. Ma, W. Liu, X. Zhu, *Adv. Mater.* **2023**, 35, 2305092.

[4] Y. Song, K. Zhang, She. Dong, R. Xia, F. Huang, Y. Cao, *ACS Appl. Energy Mater.* **2020**, 3, 7689.

[5] W. Liu, S. Sun, S. Xu, H. Zhang, Y. Zheng, Z. Wei, X. Zhu, *Adv. Mater.* **2022**, 34, 2200337.

[6] X. Xu, Q. Wei, Z. Zhou, H. He, J. Tian, H. L. Yip, Y. Fu, X. Lu, Y. Zhou, Y. Li, Y. Zou, *Adv. Funct. Mater.* **2023**, DOI: 10.1002/adfm.202305017 2305017.

[7] Y. Li, X. Guo, Z. Peng, B. Qu, H. Yan, H. Ade, M. Zhang, S. R. Forrest, *Proc. Natl. Acad. Sci. U.S.A.* **2020**, 117, 21147

[8] R. Xia, H. Gu, S. Liu, K. Zhang, H.-L. Yip, Y. Cao, *Sol. RRL* 2019, 3, 1800270

[9] Y. Li, J.D. Lin, X. Che, Y. Qu, F. Liu, L.S. Liao and S.R. Forrest, *J. Am. Chem. Soc*., 2017, **139**, 17114-17119.

[10] X. Huang, J. Oh, Y. Cheng, B. Huang, S. Ding, Q. He, F. Wu, C. Yang, L. Chen, Y. Chen, *J. Mater. Chem. A.* **2021**, 9, 5711.

[11] Y. Cui, C. Yang, H. Yao, J. Zhu, Y. Wang, G. Jia, F. Gao and J. Hou, *Adv. Mater*., 2017, **29**, 1703080. 2.

[12] S. Chen, H. Yao, B. Hu, G. Zhang, Lin. Arunagiri, L-Ku. Ma, J. Huang, Z. Zhu, F. Bai, W. Ma, H. Yan, *Adv. Energy Mater.* **2018**, 1800529.

[13] X. Ma, Z. Xiao, Q. An, M. Zhang, Z. Hu, J. Wang, L. Ding, F. Zhang, *J. Mater. Chem. A*, 2018, 6, 21485–21492.

[14] Z. Hu, J. Wang, Z. Wang, W. Gao, Q. An, M. Zhang, X. Ma, J. Wang, J. Miao, C. Yang, F. Zhang, *Nano Energy 55 (2019) 424–432.*

[15] J. Wang, J. Zhang, Y. Xiao, T. Xiao, R. Zhu, C. Yan, Y. Fu, G. Lu, X. Lu, Seth R. Marder, X. Zhan, *J. Am. Chem. Soc.* 2018, 140, 9140−9147.

[16] T. Li, S. Dai, Z. Ke, L. Yang, J. Wang, C. Yan, W. Ma, and X. Zhan, *Adv. Mater*. 2018, **30**, 1705969.

[17] Y. Li, C. Ji, Y. Qu, X. Huang, S. Hou, C.Z. Li, L.S. Liao, L.J. Guo and S.R. Forrest, *Adv. Mater*., 2019, **31**, 1903173.

[18] C. Zhu, H. Huang, Z. Jia, F. Cai, J. Li, J. Yuan, L. Meng, H. Peng, Z. Zhang, Y. Zou, and Y Li., *Sol Energy,* 2020, **204**, 660-666.

[19] J. Chen, G. Li, Q. Zhu, X. Guo, Q. Fan, W. Ma, and M. Zhang, *J. Mater. Chem. A*, 2019, **7**, 3745-3751.

[20] Q. Liu, L.G. Gerling, F. Bernal-Texca, J. Toudert, T. Li, X. Zhan, and J. Martorell, *Adv. Energy Mater*., 2020, **10**, 1904196.

[21] J. Zhang, G. Xu, F. Tao, G. Zeng, M. Zhang, Y.M. Yang, Y. Li and Y. Li, *Adv. Mater*. 2019, **31**, 1807159.

[22] Z. Yin, H. Zhao, Y. Liu, X. Xiao, Y. Zhong, H. Lai, N. Li, H. Wang, *Energy Environ. Mater.* 2024, 7, e12665.

[23] Y. Xie, L. Huo, B. Fan, H. Fu, Y. Cai, L. Zhang, Z. Li, Y. Wang, W. Ma, Y. Chen, Y. Sun, *Adv. Funct. Mater.* **2018**, 28, 1800627.

[24] H. Wang, F. Du, J. Cao, J. Yu, X. Liu, W. Tang, 10.1016/j.cej.2021.132640.

[25] Jun. Yoon, Hye. Bae, Jon. Yang, Jo-Wo. Ha, C. Lee, J. Lee, Sun. Yoon, H. Choi, Seo-J. Ko, 10.1016/j.cej.2022.139423.

[26] T. Xu, Y. Luo, S. Wu, B. Deng, S. Chen, Y. Zhong, S. Wang, G. Lévêque, R. Bachelot, F. Zhu, *Adv. Sci.* **2022**, 9, 2202150.

[27] Z. Chen, W. Ma, H. Yan, *J. Mater. Chem. A,* 2023, 11, 6901–6908.

[28] J. Jing, S. Dong, K. Zhang, Z. Zhou, Q. Xue, Y. Song, Z. Du, M. Ren, F. Huang, *Adv. Energy Mater.* **2022**, 12, 2200453.

[29] H. Chen, H. Lai, Q. Jiang, X. Lai, Y. Zhu, J. Qu, Q. Wu, F. He, *Nano Energy 113 (2023) 108593.*

[30] W. Liu, S. Sun, L. Zhou, Y. Cui, W. Zhang, J. Hou, F. Liu, S. Xu, X. Zhu, *Angew. Chem., Int. Ed.* **2022**, 61, e202116111.

[31] J. Y. Fan, Z. X. Liu, J. Rao, K. Yan, Z. Chen, Y. Ran, B. Yan, J. Yao, G. Lu, H. Zhu, C. Z. Li, H. Chen, *Adv. Mater.* **2022**, 34, 2110569.

[32] X. Duan, Y. Yang, J. Yu, C. Liu, X. Li, M. H. Jee, J. Gao, L. Chen, Z. Tang, H. Y. Woo, G. Lu, Y. Sun, *Adv. Mater.* **2024**, 36, 2308750.

[33] X. Huang, Y. Cheng, Y. Fang, L. Zhang, X. Hu, S. Y. Jeong, H. Zhang, H. Y. Woo, F. Wu, L. Chen, *Energy Environ. Sci.* **2022**, 15, 4776.

[34] L. Zhao, X. Huang, Y. Wang, S. Young Jeong, B. Huang, J. Deng, J. Liu, Y. Cheng, H. Young Woo, F. Wu, L. Chen, L. Chen, *Chem. Eng. J.* **2023**, 451, 139081.

[35] X. Huang, X. Ren, Y. Cheng, Y. Zhang, Z. Sun, S. Yang, S. Kim, C. Yang, F. Wu, L. Chen, *Energy Environ. Sci.* **2024**, 17, 2825.

[36] Y. Chang, X. Zhu, L. Zhu, Y. Wang, C. Yang, X. Gu, Y. Zhang, J. Zhang, K. Lu, X. Sun, Z. Wei, *Nano Energy 86 (2021) 106098.*

[37] Mus. Upama, Mat. Wright, Nav. Elumalai, Md. Mahmud, D. Wang, C. Xu, Ash. Uddin, *ACS Photonics* 2017, 4, 2327−2334.

[38] W. Su, Q. Fan, X. Guo, J. Wu, M. Zhang and Y. Li, *Phys. Chem. Chem. Phys*., 2019, **21**, 10660-10666.

[39] Y. Xie, R. Xia, T. Li, L. Ye, X. Zhan, H.L. Yip and Y. Sun, *Small Methods*, 2019, **3**, 1900424.

[40] B.H. Jiang, H.E. Lee, J.H. Lu, T.H. Tsai, T.S. Shieh, R.J. Jeng and C.P. Chen, *ACS Appl. Mater. Interfaces*, 2020, **12**, 39496-39504.

[41] D. Wang, R. Qin, G. Zhou, X. Li, R. Xia, Y. Li, L. Zhan, H. Zhu, X. Lu, H.L. Yip, H. Chen, C. Li, *Adv. Mater*., 2020, **32**, 2001621.

[42] P. Yin, Z. Yin, Y. Ma and Q. Zheng, *Energy Environ. Sci*., 2020, **13**, 5177-5185.

[43] N. Zhang, T. Jiang, C. Guo, L. Qiao, Q. Ji, L. Yin, L. Yu, P. Murto and X. Xu, *Nano Energy,* 2020, **77**, 105111.

[44] C. Zhu, H. Huang, Z. Jia, F. Cai, J. Li, J. Yuan, L. Meng, H. Peng, Z. Zhang, Y. Zou, and Y Li., *Sol Energy,* 2020, **204**, 660-666.

[45] Z. Hu, J. Wang, X. Ma, J. Gao, C. Xu, X. Wang, X. Zhang, Z. Wang and F. Zhang, *J. Mater. Chem. A*, 2021, **9**, 6797-6804.

[46] T. Jiang, G. Zhang, R. Xia, J. Huang, X. Li, M. Wang, H.-L. Yip and Y. Cao, *Mater. Today Energy*, 2021, **21**, 100807.

[47] X. Lu, L. Cao, X. Du, H. Lin, C. Zheng, Z. Chen, B. Sun and S. Tao, *Adv. Opt. Mater*., 2021, **9**, 2100064.